Development of High Performance UOE Pipe for Linepipe†

ARAKAWA Takekazu[*1] NISHIMURA Kimihiro[*2] YANO Koji[*3] SUZUKI Nobuhisa[*4]

Abstract:

JFE Steel manufactures high performance steels used for energy development, transportation, and storage applications. In this paper, high performance UOE pipes for linepipe manufactured from steel plates are introduced. Keywords for development are high-strengh, heavy wall thickness, high-deformability "HIPER™," collapse-resistant for deep sea, sour resistance, and low-temperature toughness. At present JFE Steel is capable of providing high-end UOE pipes in numerous sizes and for a wide range of conditions.

1. Introduction

In recent years, new customer requirements have been applied to pipelines. In addition to severe service conditions, i.e., high pressure operation and use under low temperature environments/corrosive environments, strain-based design has been adopted more widely, assuming external forces accompanying construction of long-distance pipelines in seismic areas and the sea bottom. As a result, in the pipe performance requirements demanded in pipelines, there is a heightened tendency toward addition of properties such as high strength, heavy wall thickness, low temperature toughness, high-strain capacity, and resistance to sour environments as composite specifications.

In response to this trend, JFE Steel has developed products which consider these new customer requirements through process development by strengthening its thermo-mechanical control process (TMCP) equipment for plates used as starting material for pipes, expanded application of online heat treatment process equipment (HOP™: Heat Treatment Online Process), and strengthening of the pipemaking plant, and has expanded its menu of UOE linepipe products which are capable of meeting composite specifications. **Figure 1** shows available size range of API X80 pipes (API: The American Petroleum Institute).

This paper introduces high performance UOE pipe especially for linepipe products capable of satisfying composite specifications, including (1) concept of high-strain linepipes which can be used under strain-based design (SBD) and line of high-strength and strain linepipes, (2) ultra-heavy pipes for subsea use, (3) high

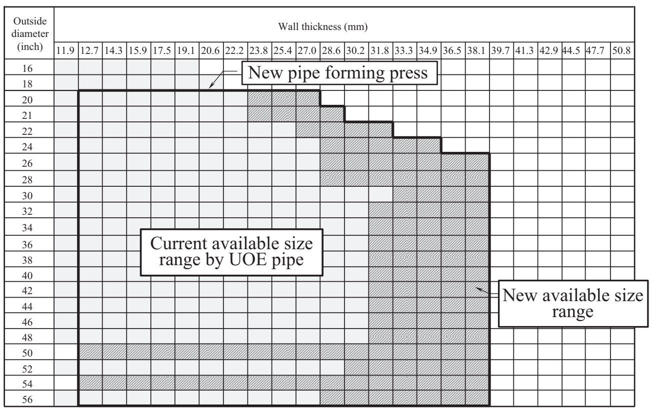

Fig. 1 API X80 Available size range (API: The American Petroleum Institute)

† Originally published in *JFE GIHO* No. 29 (Feb. 2012), p. 22–33

*1 Senior Staff General Manager,
Plate Business Planning Dept.,
JFE Steel

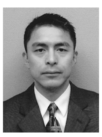

*2 Staff Deputy General Manager,
Plate Business Planning Dept.,
JFE Steel

*3 Senior Researcher Manager,
Joining & Strength Res. Dept.,
Steel Res. Lab.,
JFE Steel

*4 Senior Fellow,
Solution Div. (Kawasaki),
JFE Techno-Research

strength X80 heavy wall pipes, (4) high strength X70 steel pipes for sour service, and particularly, (5) high strength X70 heavy wall pipe with high heat affect zone (HAZ) toughness, centering on the performance of these steel pipes.

2. High-Strain Linepipe HIPER™

2.1 Basic Concept of High-Strain Linepipes

HIPER™ is a high-strain linepipe which was developed to increase the safety of high strength pipelines to the same or a higher level than pipelines of conventional strength[1–3]. With HIPER™, it is possible to improve strain capacity without increasing pipe wall thickness[1–3]. Application of HIPER™ to natural gas pipelines makes it possible to improve pipeline integrity in seismic zones and discontinuous permafrost areas while minimizing increases in construction costs[1–3]. As features of high strain pipes, since the pipe weight, transportation costs, and welding time and construction period can all be reduced, corresponding to the amount by which the pipe thickness is not increased, this is an environment-friendly product with a large CO_2 reduction effect.

Because an analytical solution predicting the critical local buckling strain under bending deformation is not required, a number of semi-empirical formulas have been proposed based on bending-buckling test data[4]. **Figure 2** shows several critical local bending-buckling strain curves calculated using representative semi-empirical formulas. The range of application of these semi-empirical formulas is X65 grade line pipe and higher. Although the semi-empirical formulas do not display individual correspondence with the test data in Fig. 2, the formulas are defined so that each of the data falls within the envelop of the lower bound and can therefore be generalized by Eq. (1). However, because Eq. (1) does not consider strain-hardening properties, it can be understood that the wall thickness must be increased in order to improve the strain capacity of the linepipe.

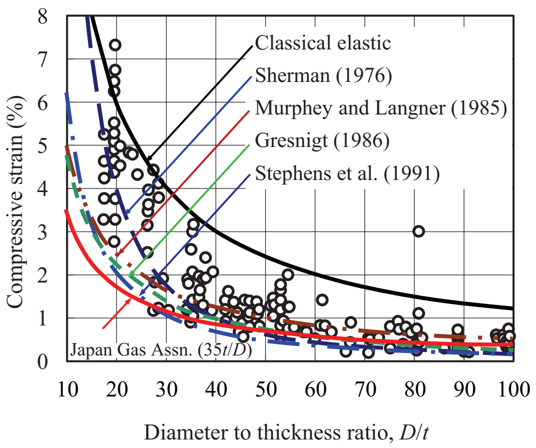

Fig. 2 Bending test results and semi-empirical formulas [1, 4]

$$\varepsilon_{cr-test} = A\left(\frac{t}{D}\right)^m \quad \cdots\cdots (1)$$

where, t: wall thickness, D: average pipe diameter. A: constant, and m: index, and are values which are obtained from test data.

In contrast to Eq. (1), semi-empirical formulas which consider strain-hardening properties will be introduced in the following. These are semi-empirical formulas that estimate the critical compressive local buckling strain and can express the strain capacity of linepipes as a function of the strain hardening parameter of the material[3].

In round-house type stress-strain curves, if the relationship of stress and total strain is expressed by the power-law function, the critical local buckling strain of a pipe under axial compression can be expressed by Eq. (2).

$$\varepsilon_{cr} = \frac{4}{3}\sqrt{n}\frac{t}{D} \quad \cdots\cdots (2)$$

where, ε_{cr}: critical local buckling strain and n: strain-hardening exponent.

If the stress-strain curve is expressed by the Ramberg-Osgood equation[5] (R-O equation), the critical local buckling strain of a pipe under axial compression can be expressed by Eq. (3)[6].

$$\varepsilon_{cr} = \frac{\sigma_0}{E}\left(\frac{\sigma_{cr}}{\sigma_0}\right) + \frac{\alpha\sigma_0}{E}\left(\frac{\sigma_{cr}}{\sigma_0}\right)^N \quad \cdots\cdots (3)$$

where, E: Young's modulus, α, σ_0, N: constants of the R-O equation, and σ_{cr}: critical compressive stress.

If the relationship between stress and plastic strain is expressed by the power-law function, the critical local buckling total strain of a pipe under axial compression can be expressed by Eq. (4), and the critical local buckling plastic strain can be expressed by Eq. (5)[7].

$$\varepsilon_{cr} = \frac{\sigma_{cr}}{E} - \frac{\sigma_0}{2E}(1+n) + \frac{4}{3}\sqrt{n}\left(\frac{t}{D}\right) \quad \cdots\cdots (4)$$

$$\varepsilon_{pcr} = \frac{4}{3}\sqrt{n}\left(\frac{t}{D}\right) - \frac{\sigma_0}{2E}(1+n) \quad \cdots\cdots (5)$$

where, ε_{cr}: critical local buckling total strain, ε_{pcr}: critical local buckling plastic strain, and E: Young's modulus, σ_0: yield stress.

Eqs. (2)–(4) are analytical solutions which predict the critical local buckling strain of a steel pipe under axial compressive deformation. Using these formulas, it is possible to obtain the strain-hardening properties which HIPER™ should satisfy for the strain demand in the structural design of pipelines. Although several additional steps are necessary to predict the critical local bending-buckling strain, Eqs. (2)–(4) are the basic formulas in the material design of high strain linepipe.

2.2 Properties of High Strain Linepipe

JFE Steel developed the high strain linepipe HIPER™ with excellent resistance to buckling by control of the dual-phase microstructure and optimization of the stress-strain curve, and has completed commercialization of grades from X52 to X100. Two types are used in control of the dual-phase microstructure, namely, the ferrite-bainite type, which is applied to grades X60-X65, and the bainite-MA type (MA: Martensite-austenite constituent), which is applied to high strength grades of X70 and higher. Typical microstructures of JFE Steel's high strain linepipe are shown in **Photo 1**. X65 grade high strain linepipe has a ferrite-bainite structure, while high strain linepipe of X80 grade displays a finer bainite-MA microstructure[8].

The anti-corrosion polymer coating is applied to linepipes. As the aging effect of heating during coating treatment increases the yield strength of the material compared to the as-UOE condition, there are cases in which mechanical properties after coating are required in high strain linepipe. With steel for bainite-MA type high strain linepipe, previous studies clarified the fact that the content of solute carbon is reduced by fine precipitation of carbides during heating by HOP™, and dislocations in the bainite are reduced by tempering; as a result, strain aging hardening is slight, and there is little change in strain capacity after coating[9]. Therefore, the bainite-MA microstructure is suitable for application to high strength pipelines of X70 and higher when coating treatment is applied.

The following presents an example of the production of high strain X80 linepipe. **Table 1** is an example of the target values of tensile properties in longitudinal direction, which were decided through consultation with the pipeline designer. These properties were calculated by the method described in the previous section based on the strain capacity required in the region where the pipelines were to be installed. The yield ratio (YR) and stress ratio were specified, and uniform elongation was also specified. The stress ratio is the ratio of stress when strain is 1.5% and stress when strain is 0.5%. The circumferential tensile specifications conform to API 5L PSL2.

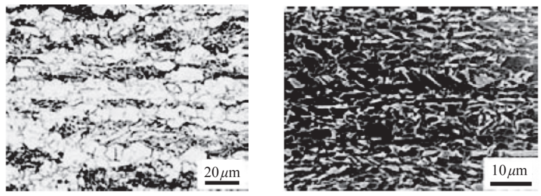

(a) API X65 Grade JFE HIPER™ (API: The American Petroleum Institute)　(b) API X80 Grade JFE HIPER™ (API: The American Petroleum Institute)

Photo 1　Examples of microstructure of high strain linepipe, HIPER™

Table 1　Longitudinal tensile specification for API X80 (API: The American Petroleum Institute) high strain linepipe

YS (MPa)	TS (MPa)	YR* (%)	$\sigma_{1.5\%}/\sigma_{0.5\%}$*	uEL* (%)
530–650	625–770	≤85	≤1.100	≥7.0

*Custumer specifications for high strain linepipe are added to API specifications.
YS: Yield strength　TS: Tensile strength　YR: Yield ratio
$\sigma_{1.5\%}/\sigma_{0.5\%}$: Stress ratio　uEL: Uniform elongation

HOP™ was applied in the plate manufacturing process with the aim of achieving a bainite-MA dual-phase microstructure with the MA fraction controlled to 5% or more in order to obtain the target stress ratio. Examples of the mechanical properties of the manufactured linepipes are shown in **Table 2**. As a coating simulation, the properties after heat treatment at 200°C × 5 min using a salt bath are also shown. Although the properties change slightly due to the aging treatment, both pipes

Table 2　Examples of mechanical properties of API X80 (API: The American Petroleum Institute) high strain linepipes

API Grade	Dimension OD (mm)	WT (mm)	Condition	Longitudinal tensile properties 1) YS (MPa)	TS (MPa)	YR* (%)	$\sigma_{1.5\%}/\sigma_{0.5\%}$*	uEL* (%)	Charpy impact test, $_vE$ at −10°C (J)	DWTT 2) SA at 0°C (%)
X80	1 219	22.0	As UOE	560	689	81	1.12	9.2	241	100
			200°C Coated	586	705	83	1.11	7.8	—	—
	1 219	26.4	As UOE	544	692	79	1.14	9.0	249	98
			200°C Coated	552	691	80	1.12	8.6	—	—

* Custumer specifications for high strain linepipe are added to API specifications.
1) Rectangular specimen
2) DWTT on 26.4 mm WT pipe was done by reduced t19 mm specimen at –11°C.
OD: Outside diameter　WT: Wall thickness　YS: Yield strength　TS: Tensile strength　YR: Yield ratio
$\sigma_{1.5\%}/\sigma_{0.5\%}$: Stress ratio　uEL: Uniform elongation　DWTT: Drop weight tear test　$_vE$: Abscrbed energy　SA: Share area

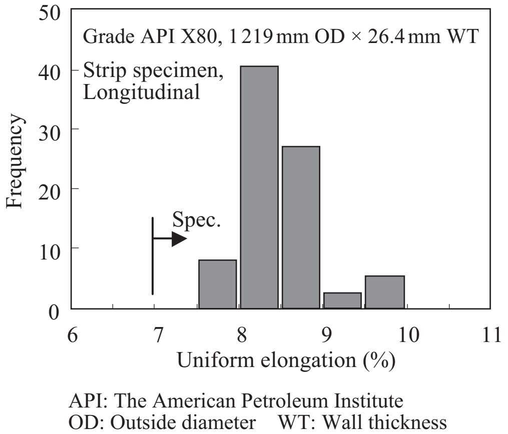

Fig. 3 Histograms of longitudinal uniform elongation

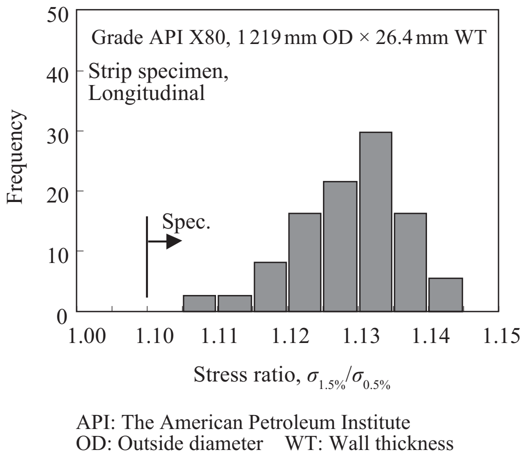

Fig. 4 Histograms of stress ratio

satisfy the specifications for high strain capacity. Furthermore, both Charpy toughness and drop weight tear test (DWTT) properties are satisfactory.

Histograms of the longitudinal uniform elongation and stress ratio of the manufactured pipes are shown in **Figs. 3** and **4**, respectively. As the target properties are amply satisfied in mass production, stable production of high strain linepipe has been realized.

3. Heavy Wall Linepipe for Deep Water Pipeline

Offshore gas pipeline development has been expanding toward deeper water region that requires pipes to have strong resistance against collapse by external pressure. The DNV standard, DNV-OS-F101 (DNV: Det Norske Veritas), is the major guideline for the design of offshore pipelines, which requires thicker wall to increase collapse resistance.

Other important material and structural parameters for controlling the collapse pressure of deepwater pipelines are compressive yield strength and roundness of the pipe. In the DNV standard, compressive yield strength is given by the tensile yield strength multiplied by the fabrication factor, α_{fab}. Fabrication factor is specified as α_{fab} = 0.85 for the linepipes manufactured by U-O-E process since the compressive yield strength is usually lower than tensile yield strength. Pre-straining of pipe body during cold forming of pipe, such as expansion process, considerably reduces yield strength in the compression test. This is because of the Bauschinger effect. Therefore, prevention of the Bauschinger effect is an important issue for enhancing compressive strength of pipes.

In addition to compressive strength, there are many other stringent material requirements for the linepipes used for deepwater pipelines. Advanced technologies in TMCP in plate manufacturing process made it possible to balance strength and toughness of heavy gauge linepipe as well as compressive strength. This chapter introduces a microstructure control for improving compressive strength while balancing other material properties. Production results of grade X65 linepipe with 36.6 mm wall thickness for offshore pipeline were also introduced.

3.1 Microstractural Factors Governing Compressive Strength of UOE Pipes

Circumferential compressive yield strength of UOE pipe is usually lower than that of tensile yield strength because of the Bauschinger effect due to the mechanical expansion applied as a final manufacturing process.

Therefore, a simple way to reduce the Bauschinger effect is to reduce the expansion rate. However, a certain level of expansion is necessary for improving roundness of the pipe. Pipe coating process, which requires heating of the pipe up to around 200°C, is also an effective way to increase compressive yield strength by strain aging[10]. Nevertheless the most reliable measure to maximize the collapse resistance of pipe is to improve the material property itself without modifying the manufacturing process.

To further increase compressive strength, it is necessary to reduce the Bauschinger effect. Since the Bauschinger effect is caused by the back stress induced by dislocation localization, obstacles against dislocation movement can cause the Bauschinger effect. Hard second phases in steel, such as cementite or martensite, increases the back stress.

Bainitic microstructure design is widely used for high strength linepipe steels, which is produced by applying controlled rolling and accelerated cooling. However, low carbon bainite often involves MA constituent, which is formed during air cooling after accelerated cooling. This hard second phase is considered to enhance the Bauschinger effect same as martensite or cementite, and need to be removed for reducing the Bauschinger effect. One of the possible measures to remove MA is to apply HOP™ process.

In order to investigate the effect of MA on the Baus-

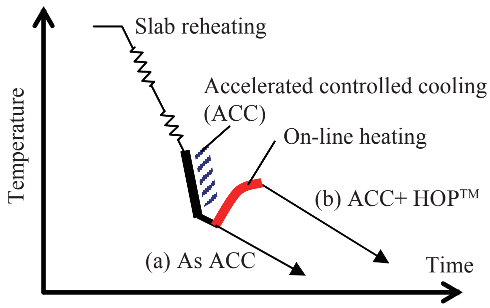

Fig. 5 Schematic illustration of thermo-mechanical control process (TMCP) conditions in plate production

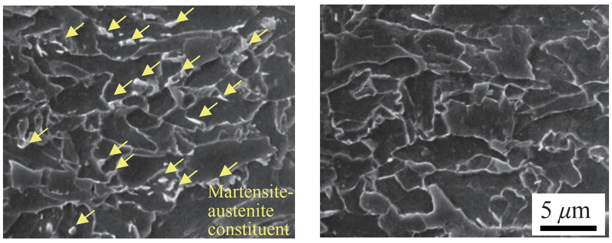

(a) As ACC (b) ACC+ HOP™

Photo 2 Microstructure of steels

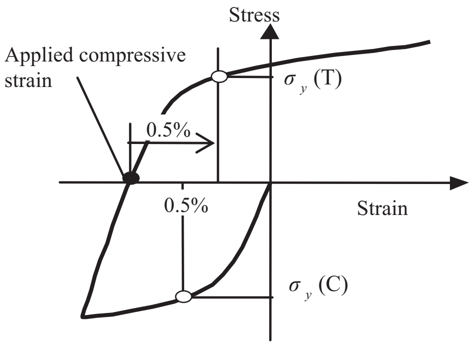

Fig. 6 Stress strain curve of Bauschinger test

chinger effect, a cyclic loading test was conducted using grade X65 plates with conventional and HOP™ process (**Fig. 5**). The chemical compositions of the steel were 0.05C-0.3Si-1.3Mn-Ni-Mo-Nb, and the plate thickness was 33 mm. The microstructure of the steel plates in the quarter thick region is shown in **Photo 2**. In the steel with the conventional process, it is seen that MA constituents, marked by arrow in the picture, are formed in the bainite matrix. On the other hand, it is clear that almost no MA was seen in the steel with the HOP™ process[11].

Round bar tensile test pieces were taken from the plates, and cyclic loading test shown in **Fig. 6** was performed. Initially, compressive pre-strain is applied, after which loading is removed and a tensile loading is applied

The steel with higher Bauschinger effect factor is considered to have higher compressive strength and to be suitable for deepwater pipeline.

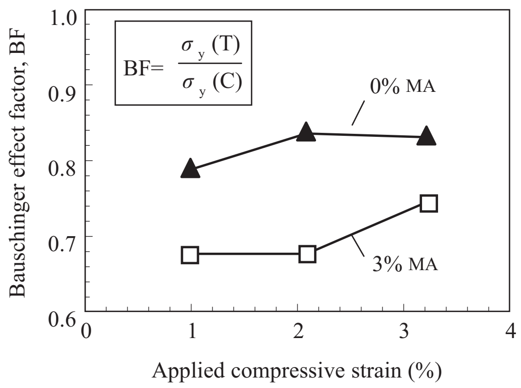

Fig. 7 Effect of martensite-austenite constituent (MA) volume fraction on Bauschinger effect factor

Bauschinger effect factor is plotted vs. compressive prestrain for both conventional and HOP™ steels in **Fig. 7**. Bauschinger effect factor for HOP™ applied steel is always higher than that of conventional steel. Even with the small volume fraction of MA in the conventional steel, MA has significant influence on the Bauschinger effect. Therefore, reducing MA is an effective measure for preventing strength reduction by the Bauschinger effect.

3.2 Manufacturing Results of Heavy Wall Linepipes

Based on the above-mentioned study, mass-production of DNV-L450 grade heavy wall linepipes was carried out. The wall thickness was 36.6 mm, and the steel plates were manufactured by applying the online heating device HOP™.

Using these steel plates, linepipes with an outer diameter of 773.2 mm were manufactured by the UOE process.The chemical compositions of the base material steel plates is shown in **Table 3**. An uniform bainitic microstructure was confirmed, and virtually no MA was observed by microstructural observation. **Table 4** shows the typical mechanical properties of the pipe. The pipe possesses strength and toughness satisfying DNV-L450 requirement, and compressive yield stress also shows a satisfactory value exceeding 90% of specified minimum yield strength (SMYS). The results of compressive strength and out-of-roundness of the pipe ends are shown in histograms in **Figs. 8** and **9**, respectively. With satisfactory higher compressive yield strength and excellent out-of-roundness as well as tensile strength and

Table 3 Chemical compositions of steels for DNV-L450 linepipe

(mass%)

Grade	C	Si	Mn	P	S	Others	Ceq
DNV-L450	0.04	0.3	1.3	0.01	0.01	Cr, Mo, Nb	0.35

DNV: Det Norske Veritas

$$\text{Cep} = \text{C} + \frac{\text{Mn}}{6} + \frac{\text{Cr} + \text{Mo} + \text{V}}{5} + \frac{\text{Cu} + \text{Ni}}{15}$$

Table 4 Typical mechanical properties of heavy wall DNV-L450 linepipe (DNV: Det Norske Veritas)

Grade	Dimension			Tensile properties[1)]			Compressive yield strength[2)] (MPa) Body 180°	Charpy impact test $_vE$ (J) at −13°C			DWTT test[3)] SA at −20°C (%)
	OD, D (mm)	WT, t (mm)	D/t	YS (MPa)	TS (MPa)	El (%)		BM	WM	FL	
DNV-L450	773.2	36.6	21.1	482	557	32	447	443	267	279	98

1)Round bar specimen (φ12.5 mm) Trans. dorection
2)ASTM E9 (φ20 mm×L60 mm) specimen (ASTM: The American Society for Testing and Materials)
3) t19 mm Reduced thickness specimen
OD: Outside diameter WT: Wall thickness YS: Yield strength TS: Tensile strength El: Elongation
$_vE$: Absorbed energy BM: Base metal WM: Weld metal FL: Fusion line DWTT: Drop weight tear test SA: Share area

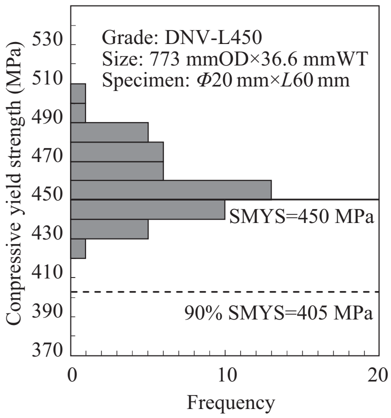

DNV: Det Norske Veritas
OD: Outside diameter WT: Wall thickness
SMYS: Specified minimum yield strength

Fig. 8 Conpression test record of heavy wall thickness linepipes

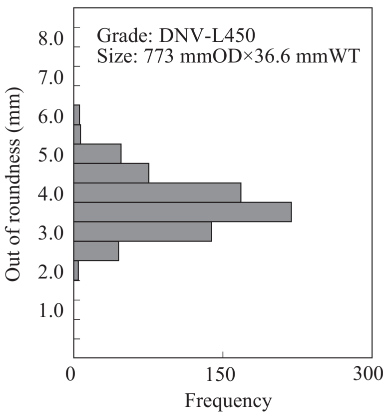

DNV: Det Norske Veritas
OD: Outside diameter WT: Wall thickness

Fig. 9 Record of out-of roundness of heavy wall thickness linepipes

toughness of pipe body and weld, these heavy gauge linepipes were proved to be suitable for subsea pipeline.

4. X80 Heavy Wall Linepipes

Accompanying the trend toward long distance pipelines, linepipes with higher strength and heavier wall thickness are now demanded from the viewpoint of high pressure operation. In the 2nd West-East Gas Pipeline in China, API 5L grade X80 linepipes with the maximum wall thickness of 26.4 mm were used in order to transport natural gas at an operating pressure of 12 MPa[12)]. In the design of pipelines for transportation of Alaskan natural gas to Canada and the United States, an ultra-high operating pressure of 17.5 MPa is being studied, and it is generally thought that heavy wall pipes of X80 will be necessary. With the trend toward heavier wall thickness products, simultaneously satisfying both strength and toughness generally becomes a difficult problem with steel materials, and the property requirements of these heavy wall thickness linepipes cannot be attained with the conventional chemical composition and manufacturing technique. Therefore, a new alloy design and plate manufacturing conditions different from the conventional method of material property control were studied, particularly for high strength linepipes with heavy wall thicknesses exceeding 30 mm. This chapter describes the study on the new alloy design and introduces grade X80 linepipes with a wall thickness of 38.1 mm which was manufactured based on the results.

4.1 Improvement of Strength and Toughness in Heavy Thickness Steel Plate

Plates for linepipes are manufactured using TMCP. In particular, accelerated cooling process is essential with high strength materials. In accelerated cooling of heavy plates, the cooling rate normally decreases as the plate thickness increases. JFE Steel developed the *Super*-OLAC™, which realizes the theoretical limit of the cooling rate by water flow control technology, and also realized the same cooling rate in heavy gauge steel plates as with thin plates produced by conventional equipment. Nevertheless, there are limits to the increase in cooling capacity when producing heavy gauge steel plates exceeding 30 mm in thickness.

Therefore, in the design of the chemical composition of plates for linepipes, addition of boron (B) was studied to improve the strength and toughness of steel plate with heavy thickness. **Figure 10** shows the results of plate rolling experiments using ingots in laboratory vacuum furnace when the amounts of various added alloying elements were changed, and with and without B addition.

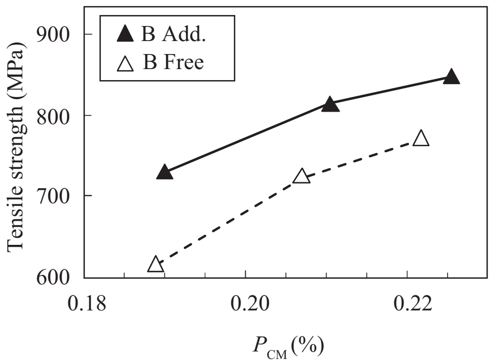

Fig. 10 Effect of boron addition on strength of thick pipe body

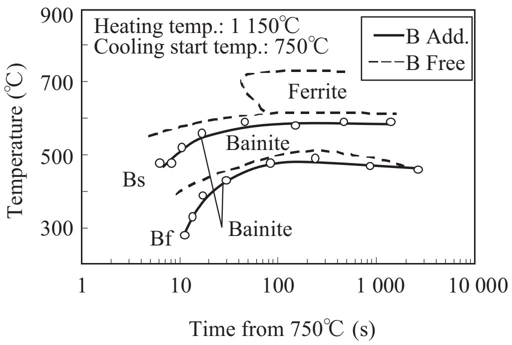

Bs: Bainite transformation start temp.
Bf: Bainite transformation finish temp.

Fig. 11 Continuous cooling transformation (CCT) diagrams of both B add. Steel and B free steel

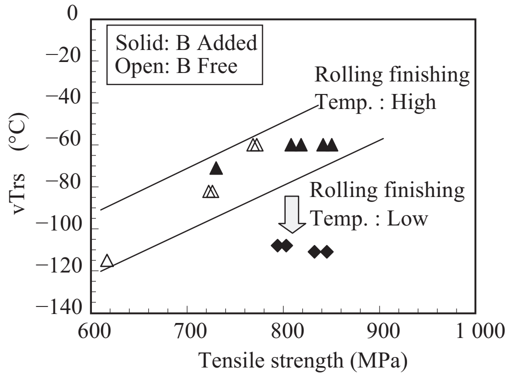

Fig. 12 Effect of thermo-mechanical control process (TMCP) condition on toughnessof thick pipe body

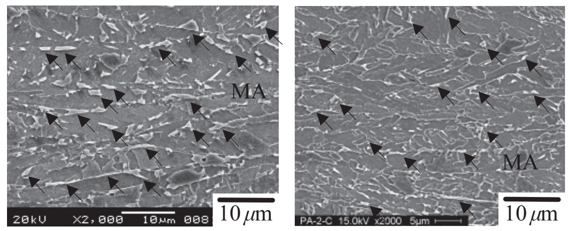

High rolling finishing temp.
MA: Volume fraction 7.5%,
Average size 3.0 μm

Low rolling finishing temp.
MA: Volume fraction 7.1%,
Average size 1.5 μm

Photo 3 Comparison of martensite-austenite constituent (MA) size in the thick pipe body between high rolling finish temp. and low one

The slabs were heated at 1 150°C and rolled. Plate rolling was finished at 780°C, followed by accelerated cooling, and finally, heating simulating the HOP™ process was applied to the rolled plate[13]. With both the B-added and B-free steel, the tensile strength of the plates increased as the weld crack parameter P_{CM} increased. However, at the same P_{CM}, higher tensile strength was obtained with the B-added steel. In other words, when the B-added composition design is used, it is possible to adopt a lower P_{CM} with the same strength grade. Therefore, it is not necessary to increase the pre-heating temperature for prevention of weld cold cracking calculated from the P_{CM} value, and excellent field weldability can also be realized.

Figure 11 shows the continuous cooling transformation diagrams (CCT diagrams) of the two types of steel, i.e., B-added and B-free, when the P_{CM} value was set at 0.21. It can be understood that the ferrite transformation in the low cooling rate range, which can be seen in the B-free steel, is suppressed by B addition, and the bainite transformation start temperature (Bs point) and finish temperature (Bf) also shift to lower temperatures. This shift to lower bainite transformation temperatures is considered to be the main factor in the increased strength of the B-added steel when ACC is applied.

Figure 12 shows the relationship between the tensile strength and the Charpy fracture appearance transition temperature (vTrs) of steel plates in a rolling experiment using B-added and B-free steels. Under the same rolling conditions, no change can be recognized in the strength-toughness ballance, irrespective of whether B is added or not. On the other hand, at the same strength, vTrs improves to the low temperature side with the B-added steels when the rolling finishing temperature is decreased. **Photo 3** shows the results of observation of the microstructures of rolled plates in the cases of high and low rolling finishing temperatures. In both cases, the bainite structure formed by transformation during accelerated cooling is the main phase, and dispersed MA formed in subsequently heating by HOP™ is observed. Photo 3 also shows the results of image analysis focusing on the distribution of the MA. Although no difference could be found in the volume fraction of MA due to the difference in the rolling finishing temperature, the average particle size of the MA becomes smaller as the finishing rolling temperature decreases. From these results, it is considered that toughness is improved through refinement of MA.

4.2 Manufacturing Results of Extra-Heavy Wall X80 Linepipes

Based on the above-mentioned study results, the chemical composition design of the heavy thickness steel plate and the plate manufacturing conditions were optimized, and grade X80 linepipes with a wall thickness of 38.1 mm were manufactured on a trial basis. The chemical composition of the steel for the pipe is shown in **Table 5**. The content of B was 0.000 7 mass%, and P_{CM} value was adjusted to 0.21 by addition of Cu, Ni, Mo, and other alloy elements. Slabs were manufactured by continuous casting and rolled to plates with a thickness of 38.1 mm by the plate rolling-*Super*-OLAC™-HOP™ process, and formed into pipes with an outer diameter of 1 216 mm by the new pipemaking equipment. The microstructure of the pipe body material is shown in **Photo 4**. The microstructure with fine dispersed MA in bainite was obtained at both the 1/4 thickness and 1/2 thickness positions, and both the strength and toughness of X80 grade requirement were achieved by the *Super*-OLAC™-HOP™ process after the low rolling finishing temperature. **Table 6** shows the mechanical properties of the pipe. The API 5L X80 standard yield strength (YS) and tensile strength (TS) were satisfied in both circumferential direction and longitudinal direction, and the pipe showed excellent deformability, i.e., L-direction YR ≦ 85% and uniform elongation ≧ 5%. In addition, the Charpy toughness and DWTT toughness showed satisfactory values at −20°C.

Table 5 Chemical compositions of steels for API X80 heavy gauge high strain linepipe (API: The American Petroleum Institute)

(mass%)

C	Si	Mn	P	S	B	Others	P_{CM}
0.06	0.04	1.9	0.01	0.001	0.000 7	Cu, Ni, Mo, Nb	0.21

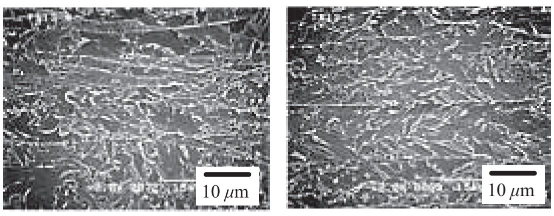

Quarter portion Center portion

Photo 4 Scanning electron microscope (SEM) micrographs of 38.1 mm thick API X80 pipe body etched by two stage electrical etching

5. Grade X70 Linepipe for Sour Service

Linepipes used in the pipeline transporting sour gas containing H_2S need to have strong resistance to hydrogen induced cracking (HIC) In order to prevent HIC, it is necessary to (1) reduce inclusions which act as crack initiation sites, (2) reduce center segregation which increases hardness and enhances crack propagation[14]. For these reasons the steel need to have higher level of cleanliness with low P and S content and addition of alloying elements such as C, Mn, and other elements are strictly controlled.

On the other hand, for the purpose of cost reduction of pipeline construction and operation, higher grade linepipes for sour service are expected. To achieve higher strength over grade X65 steels need to have richer chemistries, but this invites the formation of hard second phase such as MA which in turn increases susceptibility to HIC[15].

This chapter introduces the development of a new TMCP technology for achieving high strength exceeding X65 with a homogeneous microstructure without hard MA phase and trial production result of grade X70 UOE linepipe for heavy sour application by applying the state of the art technology

5.1 Microstructure Control for Improved HIC Resistance

In order to produce such a high strength and high performance linepipe steels, JFE Steel developed the online heat treatment process HOP™.[16] Combination with *Super*-OLAC™ and HOP™ has enabled novel metallurgical controlling that cannot be achieved by the conventional TMCP process. Material design concepts for sour resistant linepipe steel are: (1) transformation strengthening by homogeneous and fine bainitic microstructure obtained through higher cooling rate with *Super*-OLAC™ by accelerated cooling, (2) promoting precipitation of alloy carbides by rapid heating immediately after accelerated cooling, and (3) preventing MA

Table 6 Mechanical properties of 38.1mm thick API X80 linepipe (API: The American Petroleum Institute)

Grade	Dimensions		Tensile properties[1]					Charpy impact test		DWTT
	OD (mm)	WT (mm)	Direction	YS, Y (MPa)	TS, T (MPa)	Y/T ratio (%)	Elongation (%)	Direction	${}_vE_{-20}$ ave. (J)	SA at −20°C[2] ave. (%)
API X80	1 219	38.1	Trans.	600	765	78	45	Trans.	131	85
			Longi.	605	744	81	47			

[1]Rectanglar specimen [2]Full thickness specimen
OD: Outside diameter WT: Wall thickness YS: Yield strength TS: Tensile strength ${}_vE_{-20}$: Absorbed energy at −20°C
DWTT: Drop weight tear test SA: Share area

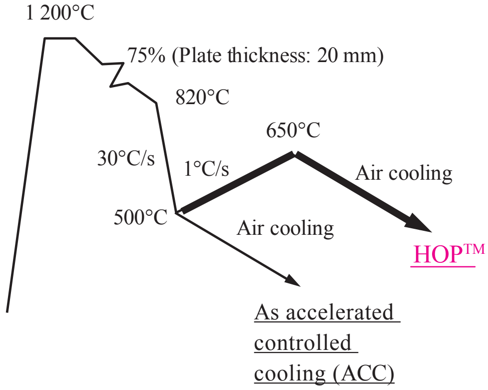

Fig. 13 Schematic illustration of laboratory hot rolling conditions

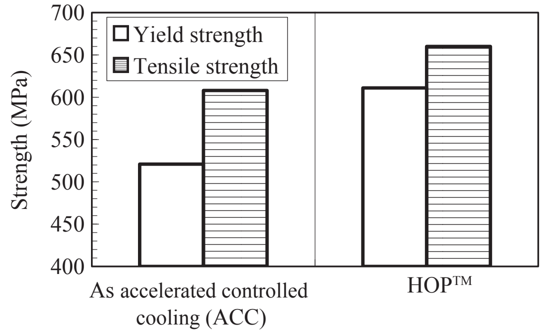

Fig. 14 Tensile properties of the steels

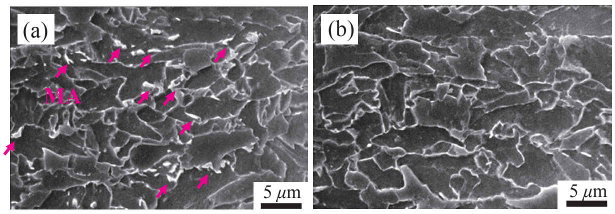

(a) As accelerated controlled cooling (ACC)

(b) HOP™

Photo 5 Scanning electron microscope (SEM) micrographs of the steels etched by two stage electrical etching

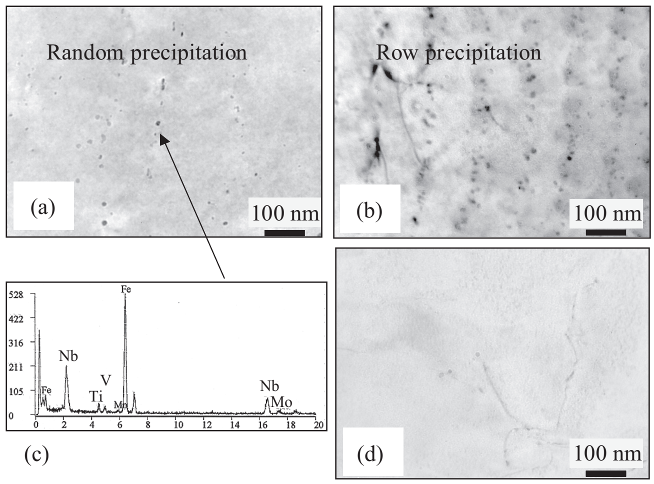

Fig. 15 Transmission electron microscope (TEM) analysis results of the steels ((a), (b): Micrograph of HOP™, (c) Energy dispersive x-ray spectroscopy (EDX) profile of HOP™, sprecipitates, (d) Micrograph of as accelerated controlled cooling (ACC))

formation by reducing carbon enrichment during bainitic ferrite transformation.

Using a 0.05C-1.25Mn-0.1Mo-0.04Nb-0.045V-Ti steel, verification was performed by conducting a laboratory experiment under the TMCP conditions shown in **Fig. 13**. Laboratory rolling was performed at two levels, one under the conventional accelerated controlled cooling conditions (as-accelerated controlled cooling (ACC) material), and the other, under the above-mentioned conditions applying the HOP™.

Photo 5 shows the microstructures of the respective laboratory rolled materials. In the as-ACC steel, the results of scanning electron microscope observation after 2-stage electrical etching confirmed the existence of MA, which is visible as a white grain-like form in the bainite matrix. In contrast, virtually no MA was observed in the HOP™ steel. **Figure 14** shows the results of a tensile test of the laboratory-rolled steel. In comparison with the as-ACC steel, the HOP™ steel shows about 80 MPa higher YS and approximately 50 MPa higher TS. **Figure 15** shows the results of transmission electron microscope observation. In the HOP™ steel, a large number of precipitates were observed in two modes of precipitation, i.e., random precipitation (Fig. 15(a)) and row precipitation (Fig. 15(b)). From the results of composition measurement by energy dispersive X-ray spectroscopy (EDX) shown in Fig. 15(c), the precipitates are considered to be complex carbides of Nb, Ti, Mo, and V. On the other hand, the as-ACC steel displayed only tiny amounts of coarse (Nb, Ti) and (C, N), which were not dissolved during slab heating and hot rolling (Fig. 15(d)), and precipitation of finer alloy carbides was not observed.

Experimental results demonstrated that prevention of MA formation and precipitation strengthening can be achieved by the new TMCP process using HOP™. which can be applied to higher grade linepipe steel for sour service.

5.2 Manufacturing Results of Grade X70 Linepipe for Sour Service

Based on the results described above, API 5L grade X70 linepipes with sour resistance were manufactured using steel plates by applying the technology for uniform microstructure control in the plate thickness direction to reduce susceptibility to HIC. The pipe wall thickness was 19.1 mm. Plates were manufactured using the online heating device HOP™, and linepipes with an outer diameter of 914.4 mm were manufactured by the UOE process.

The chemical composition of the steel plates is shown in **Table 7**. The contents of C, P, and Mn were the same as the conventional X65 steel for sour service, and a lower alloying design than the conventional non-sour X70 linepipe was adopted, namely, a P_{CM} value of 0.14. Microstructure observation confirmed that the base material had a homogeneous bainitic microstructure without MA. **Figure 16** shows the hardness distribution in the width direction of the plate. From the edge to the center, hardness differences were extremely small, as the Vickers hardness at the plate surface and 1/4 thickness position was 180–200 points. This demonstrates the homogeneous material properties throughout the plates. **Table 8** shows examples of the mechanical properties of the pipe. The developed linepipe has enough strength which satisfies the API 5L X70 standard, and satisfactory properties were also obtained in the Charpy impact test and the DWTT test. For the HIC property, a 96-hours immersion experiment was performed under a condition of 100% H_2S gas saturation of solution A as specified in NACE TM0284 (NACE: The National Association of Corrosion Engineers). The results showed excellent HIC resistance, in which no cracking was found in all cases.

Table 7 Chemical compositions of sour resistant API X70 (API: The American Petroleum Institute) UOE pipe

(mass%)

Grade	Chemical compositions						
	C	Si	Mn	P	S	Others	P_{CM}
API X70	0.05	0.28	1.13	0.014	0.000 5	Mo, Ni, Cr, Nb, Ca	0.14

P_{CM} = C+Si/30+Mn/20+Cu/20+Ni/60+Cr/20+Mo/15+V/10+5B

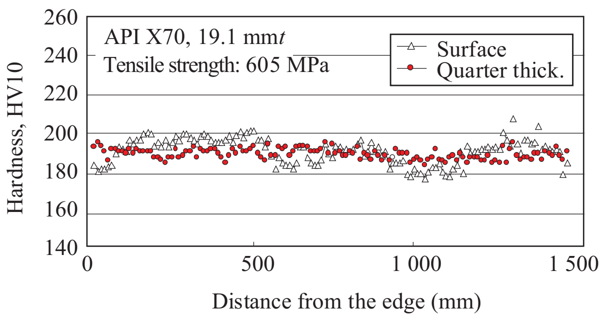

Fig. 16 Hardness distributions along the plate width of sour API X70 (API: The American Petroleum Institute) steel plate

Table 8 Mechanical and sour properties of sour API X70 (API: The American Petroleum Institute) UOE pipes

Pipe number	Tensile properties[1)]				Impact property	DWTT	HIC[2)]	
	YS, Y (MPa)	TS, T (MPa)	EL (%)	Y/T (%)	$_vE$ (J) at −10°C	SA at 0°C (%)	CLR (%) 90°	CLR (%) 180°
1	531	613	23	87	373	100	0, 0, 0	0, 0, 0
2	523	600	22	87	343	100	0, 0, 0	0, 0, 0

1) ISO lecutanglar specimen, trans. direction
2) NACE TM0284-solution A (NACE: The National Association of Corrosion Engineers)
YS: Yield strength TS: Tensile strength
El: Elongation $_vE$: Absorbed energy
DWTT: Drop weight tear test SA: Share area
HIC: Hydrogen-induced cracking CLR: Crack length ratio

6. Heavy Wall Thickness X70 UOE Linepipe for Low Temperature Service

6.1 Issues of Seam Welding of Heavy Wall Thickness UOE Pipes

Accompanying high pressure operation of pipelines and use in deep waters, pipes with high strength and heavy wall thickness are being adopted. Under these conditions, pipes having high HAZ toughness are required, even in X70 heavy wall thickness pipes. Therefore, it is necessary to obtain both of high strength by means of addition of alloying elements and high HAZ toughness in the as-welded condition in thick wall double-side submerged arc welded pipes (DSAW

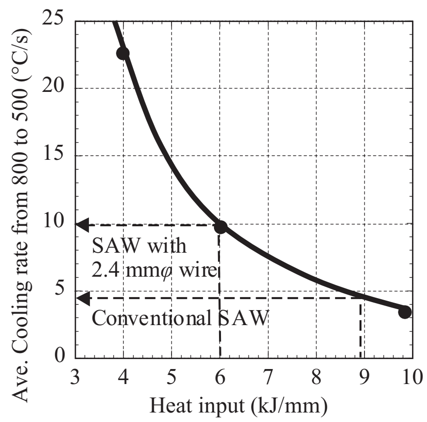

SAW: Submerged arc welding

Fig. 17 Relationship between heat input and cooling rate (Wall thickness: 33.0 mm, Ave. of inside weld and outside weld)

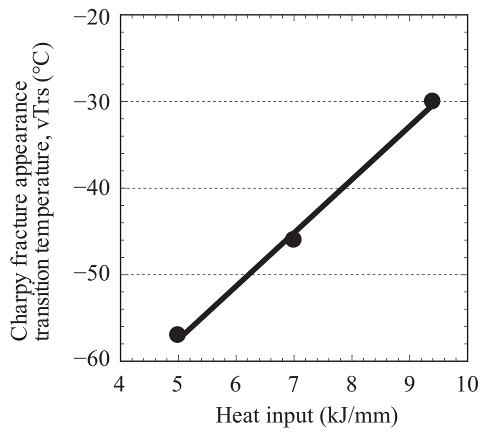

Fig. 18 Relationship between heat input and heat-affected zone (HAZ) toughness (API X70, 4 Electrodes Submerged arc welding (SAW))

pipes)[17]. Preventing increase in heat input in seam welding is an effective means of improving HAZ toughness. **Figure 17** shows the relationship between the heat input in welding of steel pipes with a wall thickness of 33 mm and the weld cooling rate (800–500°C). Under the conventional submerged arc welding (SAW) conditions, the average heat input of the inside and outside welds is 8.8 kJ/mm, and the weld cooling rate is slow, at approximately 4.0°C/s.

Reduction of the cooling rate accompanying increased welding heat input has negative effects on HAZ toughness[18], as it expands the toughness deterioration region comprising the coarse grain heat affected zone (CGHAZ) and intercritically reheated coarse grain heat affected zone (ICCGHAZ), and also causes coarsening of the prior austenite (γ) grain size[19,20]. **Figure 18** shows the effect of welding heat input on HAZ toughness of X70 welded joint (Thickness: 33.0 mm). As heat input decreases, vTrs decreases, and HAZ toughness improves.

6.2 Low Heat Input SAW Technology Applying Smaller Diameter Welding Wire

As a technique for reducing heat input, a low heat input SAW technology using a smaller diameter welding wire as the leading electrode was developed[21,22], improving HAZ toughness in seam welds of heavy wall thickness X70.

The following may be mentioned as effects of using the smaller diameter welding wire as the leading electrode: (1) a high deposition rate can be obtained as a result of the increase in Joule heating accompanying the increased electrical resistance of the smaller diameter wire[23], and (2) arc energy density is increased by the higher current density, and simultaneously with this, the arc is focused by the electromagnetic pinch force and a deeper weld penetration depth can be obtained[24].

Figure 19 shows the effect of the wire diameter on the wire deposition rate with wires having diameters of 1.6 mm to 4.0 mm. In seam welding of UOE pipes, wires with diameter of 4.0 mm or 4.8 mm are generally used. However, the wire deposition rate is greatly increased by using a smaller diameter welding wire, and the effect of the smaller diameter wire is remarkable on the large current region.

Figure 20 shows the effect of the wire diameter on the penetration depth with wires of 1.6 mm to 4.8 mm in diameter. Penetration increases when smaller diameter wires are used, and the deepest penetration is obtained with a wire diameter of 2.4 mm or smaller.

Based on the results described above, a 2.4 mm in diameter wire was adopted as the leading electrode because it is possible to use of the large current with this welding technology and this size has a large effect in

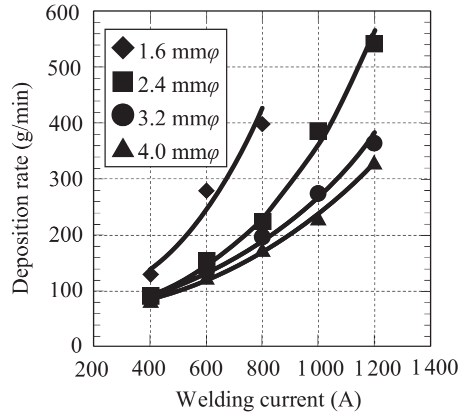

Fig. 19 Relationship between wire diameter and deposition rate (Single electrode, Bead on plate, 35 V-60 cm/min)

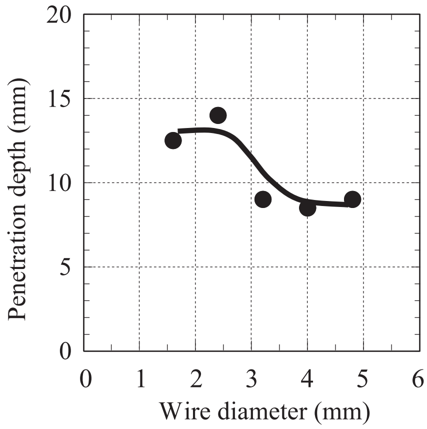

Fig. 20 Relationship between wire diameter and penetration depth (Single electrode, Bead on plate, 800 A-35 V-60 cm/min)

increasing the penetration depth and wire deposition rate. This small-diameter wire SAW technology enables welding with a smaller heat input than the conventional SAW technology. Moreover, the effect of heat input reduction becomes larger as the wall thickness increases.

To clarify the effect of this small-diameter wire SAW technology in improving HAZ toughness, welded joints of X70 (33.0 mm*t*) were prepared experimentally using the small-diameter wire SAW technology, and the properties of the welds were evaluated. **Table 9** shows the welding conditions. In comparison with the conventional method, the welding heat input was reduced by approximately 30% as the total of the inside and outside welds.

The cooling rate of the weld metal with the conventional method was approximately 4°C/s, but in contrast, that increases to approximately 10°C with small-diameter wire SAW. **Photo 6** shows the CGHAZ microstructure around the fusion line at a depth of 7 mm below the surface layer of the outside weld metal. Accompanying the reduction of heat input, the prior γ grain size of the CGHAZ is refined. **Table 10** shows the results of a HAZ Charpy test of the outside weld fusion line and the root fusion line (intersection of the inside

Table 9 Welding condition of laboratory evaluation

	Inside weld/ Outside weld	Wire Diameter of lead electrode (mm)	Travel speed (mm/min)	Heat input (kJ/mm)
Conventional SAW	IW	4.0	1 050	8.2
	OW	4.0	910	9.4
SAW with 2.4 mmφ wire	IW	2.4	1 670	5.0
	OW	2.4	1 200	7.0

SAW: Submerged arc welding

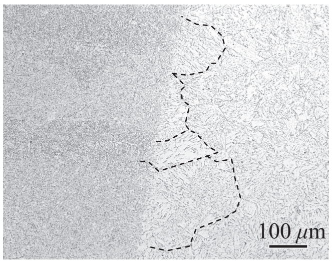

(a) Conventional SAW

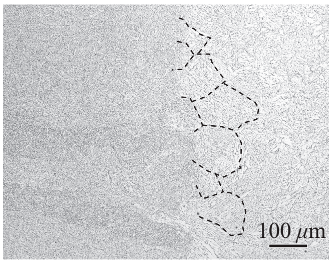

(b) SAW with 2.4 mmφ wire

SAW: submerged arc welding

Photo 6 Coarse grain heat-affected zone (CGHAZ) microstructure of API X70 (33.0 mm*t*)

Table 10 Charpy impact test results

	Absorbed energy at −30°C, $_{\mathrm{v}}E_{-30}$ (J, Ave. of n=3)	
	Outside weld (OW) fusion line	Root fusion line
Conventional SAW	106	125
SAW with 2.4 mmφ wire	191	205

SAW: Submerged arc welding

Table 11 Welding condition of trial production

Inside weld/ Outside weld	Wire diameter of lead electrode (mm)	Travel speed (mm/min)	Heat input (kJ/mm)
IW	4.0	950	4.5
OW	2.4	1 250	6.3

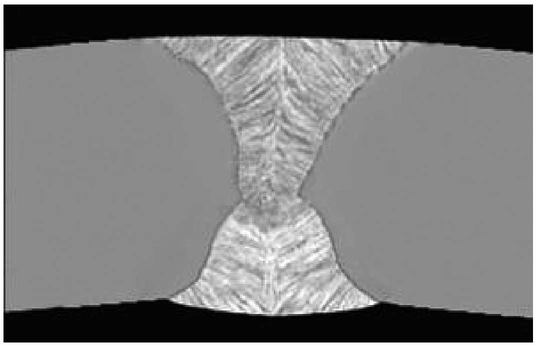

Photo 7 Penetration depth of 30.9 mm*t*

Table 12 Mechanical property test results of trial production of API X70 (30.9 mm*t*)

Pipe body					
Tensile test C-direction		DWTT −10°C	$_{\mathrm{v}}E_{-30°C}$ (n=3)		CTOD −10°C (mm)
YS (MPa)	TS (MPa)	SA (%)	Ave. (J)	Min. (J)	
564	660	96 100 100 100	214	187	0.660 0.316 0.585

Seam HAZ (Fusion line)						
$_{\mathrm{v}}E_{-30°C}$ (n=6)						CTOD −10°C (mm)
Outside weld		Root		Inside weld		
Ave. (J)	Min. (J)	Ave. (J)	Min. (J)	Ave. (J)	Min. (J)	
173	141	151	101	230	227	0.431 0.268 0.592

YS: Yield strength TS: Tensile strength
DWTT: Drop weight tear test SA: Share area
$_{\mathrm{v}}E_{-30°C}$: Absorbed energy at −30°C
CTOD: Crack tip opening displacement
HAZ: Heat-affected zone

and outside weld fusion lines). Improvement of HAZ toughness by heat input reduction was confirmed with small-diameter SAW.

6.3 Manufacturing Results of Heavy Wall Thickness X70 UOE Linepipe

Heavy wall thickness X70 UOE pipes (30.9 mm*t*) for low temperature service were manufactured on a trial basis applying the small-diameter wire SAW technology to seam welding. The welding conditions, a macrograph of the weld cross section, and the results of mechanical property tests are shown in **Table 11**, **Photo 7**, and **Table 12**, respectively. Sound welds with satisfactory lap of the inside weld bead and outside weld bead were obtained by application of the small-diameter wire SAW technology, and it was possible to manufacture pipes having excellent HAZ toughness of $_{\mathrm{v}}E_{-30} \geqq 100$ J in the Charpy tests of the inside weld, outside weld, and root fusion lines.

7. Conclusion

This paper introduced products developed by JFE Steel in response to new customer requirements for steel pipes for linepipes in recent years, using JFE Steel's TMCP technology for steel plates used as materials for those pipes and steel pipe manufacturing technologies. Focusing on the keywords of high strength, heavy wall thickness, low temperature toughness, high deformability, and sour resistance, the lineup of products which is capable of meeting composite specifications for those properties was described.

In the future, JFE Steel will continue to develop steel plates and steel pipes for linepipes in response to increasingly advanced and diverse requirements by concentrating its steelmaking, plate manufacturing, and UOE pipemaking technologies, taking advantage of its distinctive features as an integrated steel maker, and will contribute to the development of the energy industries which the world demands by supplying outstanding steel products which are also environment-friendly.

References

1) Suzuki, Nobuhisa; Igi, Satoshi; Masamura, Katsumi. Seismic integrity of high-strength pipelines. JFE Technical Report. 2008, no. 12, p. 1–7.
2) Suzuki, Nobuhisa; Kondo, Joe; Shimamura, Junji. Strain capacity of high-strength line pipes. JFE Technical Report. 2008, no. 12, p. 20–26.
3) Suzuki Nobuhisa. Goal-setting design to ensure integrity of high-strength and large diameter pipeline. Jour. of the Jpn. Welding Soc. 2011, vol. 80, no. 3, p. 253–260.
4) Zimmerman, T. J. E.; Stephens, M. J.; DeGeer, D. D.; Chen, C. Compressive Strain Limits for Buried Pipelines. 1995 OMAE. vol. 5, Pipeline Technology, p. 365–378.
5) Ramberg, W.; Osgood, W. R. Description of Stress-Strain Curves by Three Parameters. NACA. 1943, TN, 902.
6) Suzuki, N.; Toyoda, M. Critical Compressive Strain of Linepipes Related to Work-Hardening Parameters. Proc. of the 21st Int. Conf. on OMAE. 2002, paper no. OMAE2002–28253.
7) Suzuki, N.; Zhou, J.; Toyoda, M. Compressive Strain Limits of High-Strength Linepipes. Proc. of the 7th Int. Pipeline Conf., 2008, paper no. IPC2008-64526.
8) Ishikawa, Nobuyuki; Endo, Shigeru; Kondo, Joe. High performance UOE linepipes. JFE Technical Report. 2006, no. 7, p. 20–26.
9) Okatsu, Mitsuhiro; Shikanai, Nobuo; Kondo, Joe. Development of a high-deformability linepipe with resistance to strain-aged hardening by HOP (Heat-treatment On-line Process). JFE Technical Report. 2008, no. 12, p. 8–14.
10) DeGeer, D. et al. 2004, OMAE2004–51569.
11) Ishikawa, Nobuyuki; Shinmiya, Toyohisa; Sueyoshi, Hitoshi; Shikanai, Nobuo. Effect of hard second-phase on bauschinger effect of low carbon high strength steels. CAMP-ISIJ. 2008, vol. 21, p. 1409.
12) Muraoka, R. et al. IPC2010–31556, 2010.
13) Okatsu, M. et al. OMAE2005–67149, 2005.
14) Taira, T.; Tsukada, K.; Kobayashi, Y.; Tanimura, M.; Inagaki, H.; Seki, N. Nippon Kokan Techical Report Overseas. 1981, no. 31, p. 1–13.
15) Endo, S.; Doi, M.; Ume, K.; Kakihara, S.; Nagae, M. Proceedings of 38th MWSP Conference. ISS. 1997, vol. 34, p. 535–541.
16) Fujibayashi, Akio; Omata, Kazuo. JFE Steel's advanced manufacturing technologies for high performance steel plates. JFE Technical Report. 2005, no. 5, p. 10–15.
17) Schwinn, V.; Parunov, A.; Bauer, J.; Stepanov, P. "SAWL 485 for 48" Offshore Application in Thickness up to 41 mm." Proceedings of IPC2008 7th International Pipeline Conference. 2008.
18) Inagaki, Michio; Nakamura, Harumasa; Okada, Akira. Jour. of the Jpn. Welding Soc. 1965, vol. 34, no. 10, p. 1064.
19) Nakao, Y.; Oshige, H.; Noi, S.; Nishi, Y. "Distribution of Toughness in HAZ of Multi-Pass Welded High Strength Steel." Quarterly Journal of the Japan Welding Society. 1985, vol. 3, no. 4, p. 773–781.
20) Graf, M.; Niederhoff, K.; Pipeline Technology Conference. Ostend, Belgium, 1990, part B, p. 13.
21) Ishigami, A.; Murakami, Y.; Hayakawa, N.; Tanizawa, A. "Development of Heavy Wall High-Strength UOE Linepipe by Means of Microstructural Control in Base Metal and Seam Weld." Proc. OMAE 2011. paper OMAE2011–50312.
22) Ishigami, A.; Hayakawa, N.; Yano, K.; Endo, S. Development of low heat input submerged arc welding. Preprints of the National Meeting of the Jpn. Welding Soc. 2011, no. 89, p. 364–365.
23) Halmoy, E. Proc. Arc Physics and Weld Pool Behaviour. TWI London, 1979.
24) Herbst, H. T.; McElrath, T. Sigma Welding of Carbon Steels. J. A. W. S., 30, 1084, 1951